# AJNR

**Fast spin-echo MR imaging of the cervical spine: influence of echo train length and echo spacing on image contrast and quality.**

G Sze, Y Kawamura, C Negishi, R T Constable, M Merriam, K Oshio and F Jolesz

# Fast Spin-Echo MR Imaging of the Cervical Spine: Influence of Echo Train Length and Echo Spacing on Image Contrast and Quality

Gordon Sze,[1] Yasutaka Kawamura,[1] Chikashi Negishi,[1] R. Todd Constable,[1] Michael Merriam,[1] Koichi Oshio,[2] and Ferenc Jolesz[2]

**PURPOSE:** To examine the interaction of echo train length and interecho spacing and their effects on image quality and contrast in fast spin-echo sequences of the cervical spine. **METHODS:** Forty-three patients with suspected cervical disk disease were prospectively evaluated with fast spin-echo with varying echo train lengths and interecho spacing. A flow phantom was used to confirm findings related to cerebrospinal fluid pulsation. Parameters were manipulated to adjust contrast, signal-to-noise ratio, the effects of artifacts, and the speed of acquisition. **RESULTS:** In general, increasing echo train length increased homogeneity and high intensity of cerebrospinal fluid signal and reduced acquisition time; however, it decreased the signal-to-noise ratio of cerebrospinal fluid and cord and increased blurring, and, to a lesser extent, edge enhancement, and "truncation-type" artifact. Increasing interecho space permitted the use of longer echo times but minimally decreased contrast and signal-to-noise ratio of cord and cerebrospinal fluid. In addition, increasing echo spacing increased blurring, edge enhancement, truncation-type, magnetic susceptibility, and motion artifacts. **CONCLUSIONS:** For cervical spine imaging, a long echo train length and short echo spacing partially compensate for cerebrospinal fluid flow and produce the best myelographic effect but must be modulated by other constraints, such as artifact production or technical capabilities.

**Index terms:** Magnetic resonance, comparative studies; Magnetic resonance, technique; Spine, intervertebral disks, degeneration; Spine, magnetic resonance

Fast spin-echo (FSE) sequences based on the original RARE (rapid acquisition with relaxation enhancement) sequence (1–7) now have the potential to produce high-quality images with high-intensity cerebrospinal fluid (CSF) in a shorter time than either gradient-echo or conventional spin-echo (SE) sequences and with less magnetic susceptibility artifact, which often causes overestimation of degenerative changes (8). The development of FSE sequences, however, introduces new factors that must be considered in adapting this technique to clinical use (5–6). First, in addition to repetition time (TR) and echo time (TE), new parameters, such as echo train length and interecho spacing, also can affect image contrast and resolution through their influences on the order in which k-space is sampled. Second, FSE sequences are susceptible to a new set of artifacts, such as image blurring secondary to nonuniform sampling of k-space. Third, conventional solutions to compensate for CSF pulsation, such as cardiac gating and gradient moment nulling, either prolong imaging time (cardiac gating) or may limit the range of other parameters (gradient moment nulling).

An understanding of the appearance of CSF flow on FSE imaging becomes necessary. In the evaluation of suspected cervical degenerative disease, adequate anatomic detail, especially as outlined by high-intensity CSF, remains crucial. Detailed understanding of the influence of echo train length and echo spacing is essential in the application of the new FSE sequences to imaging of the cervical spine.

TABLE 1: FSE pulse sequence parameters—sagittal

| Group (no. of patients) | TR (msec) | TE (msec) | Echo Train Length | Echo Spacing (msec) | Time of Scan |
|---|---|---|---|---|---|
| 1 (12) | 2000 | 20 or 80 | 4, 8, 12, 16 | 20 | 52 sec to 3 min 16 sec. |
| 2 (11) | 2000 | 14–22, 120–132 | 16 | 14, 16, 18, 20, 22 | 52 sec |

TABLE 2: FSE pulse sequence parameters—axial

| Group (no. of patients) | TR (msec) | TE (msec) | Echo Train Length | Echo Spacing (msec) | Time of Scan |
|---|---|---|---|---|---|
| 1 (10) | 2000 | 126 | 8, 12, 16 | 18 | 4 min 18 sec to 8 min 36 sec |
| 2 (8) | 2000 | 14–30 or 120–130 | 16 | 14, 16, 18, 20, 24, 26, 28, 30[a] | 4 min 18 sec |

[a] 28 mses was not compatible with the long TE range.

## Materials and Methods

The study of the effects of echo train length and echo spacing on image quality was performed prospectively in a fashion similar to that carried out in previous studies for gradient-echo imaging of the spine (9–11). CSF motion strongly influences relevant tissue contrast but is difficult to model in theoretical calculations because of its pulsatility (9). Thus, this investigation was conducted clinically. Further verification of findings was sought with a flow phantom.

Forty-three patients with suspected cervical degenerative change were prospectively studied at 1.5 T. Cooperative patients were accrued consecutively within the constraints of scheduling. A cervical spine receive-only posterior surface coil was used to obtain 3-mm sections. The generic FSE pulse sequences consisted of a single 90° radiofrequency pulse, followed by multiple 180° pulses, the exact number of which constituted the echo train length. The spacing between successive echoes formed the echo spacing. Each echo was individually phase encoded before readout. In order to eliminate residual phase, phase was unwound after each echo. We selected the smallest TE at which the smallest phase-encoding gradient was applied, because signals acquired with these low spatial ($k_y$) frequencies controlled image contrast.

The FSE sequences used in the study differed in the sagittal and axial planes. For reasons similar to those in gradient-echo imaging, a two-dimensional Fourier transform (2DFT) technique was used in the sagittal plane and a 3DFT technique in the axial plane (12). Both sequences have been described previously (6, 7). The 3DFT sequence was a multislab technique in which four slabs were excited with each slab phase encoded into eight sections in the section-slab direction. The multislab approach was chosen because it permitted data acquisition in each slab sequentially during a single TR, resulting in four z-phase-encode steps, thus speeding up the sequence fourfold. Further modifications allowed placement of the lowest order phase-encoding step at any echo of the echo train. All of the $k_y$ phase-encode steps were collected at one $k_z$ step before $k_z$ was incremented. Twenty-four contiguous sections of 3 mm were obtained after the end sections of each slab were discarded.

In all cases, two excitations were used in the 2DFT FSE sequences and one in the 3DFT FSE sequences. All sequences were performed as single-echo acquisitions to permit greater flexibility of parameter manipulation. The phase-encoding axis lay in the y axis in the 2DFT sequences and in the y- and z-axes in the 3DFT sequences. The bandwidth was ±32 kHz, allowing narrower interecho spacing and decreasing chemical shift effects compared with the standard ±16 kHz bandwidth. The matrix was 256 × 192 in all sagittal acquisitions and 256 × 192 or 256 × 256 in all axial acquisitions. Gradient moment nulling was not used initially, because it can limit the range of some parameters, especially echo spacing. Rather, parameters were first studied to understand their effects on image quality; gradient moment nulling was then applied to these optimized parameters.

Patients with suspected cervical extradural disease were prospectively studied. They were divided into two groups. The echo train length or interecho spacing of each group was varied, whereas the other parameter was held fixed (in certain ranges). A summary of the parameters is given in Tables 1 and 2.

FSE images were analyzed quantitatively and qualitatively. Quantitatively, intensity measurements of spinal cord, CSF, and disk (or ligament) were performed by defining a region of interest at least 5 pixels in size with a user-interactive cursor. All regions of interest were selected adjacent to each other in order to minimize signal fall-off from the coil. All intensities were measured three separate times for each structure by delineating different regions of interest. These measurements were then averaged to obtain the final result. Noise calculations were obtained according to standard methodology, and the mean signal intensity of air, the standard deviation, and the area of measurement were noted (13, 14). Signal-to-noise ratios (SNRs) of CSF and cord were calculated. Contrast was also calculated for CSF to cord or CSF to disk according to the following equation:

$$\text{Contrast} = [\text{CSF} - \text{cord (disk)}] \div \text{cord (disk)}.$$

Qualitatively, the multiple FSE images with varying parameters were compared with each other and were examined for the detectability of extradural disease, the quality

of the myelographic effect, and the presence of artifact, such as CSF pulsation, magnetic susceptibility, blurring, or edge enhancement. In order to evaluate the images, three criteria were chosen. First, the ability to detect and delineate pathology was examined. Second, if scans were judged equal in detection and delineation of pathology, then overall image quality was considered. Particular attention was paid to optimizing homogeneity of the CSF signal. Third, if all other criteria were equal, then the speed of the scan was the final consideration.

In order to verify the findings suggested from the prospective clinical studies, a flow phantom was constructed using a pump (Signet Scientific, El Monte, CA), 3/4-inch diameter tubing, and a solution of water and $MnCl_2$ adjusted to have a T1 relaxation time of approximately 500 msec. The fluid was pumped at a steady rate through the tubing, which was either placed in a control bath or next to a container of control solution. Although actual CSF flow is pulsatile and to-and-fro, the phantom was felt to be a simple controlled model showing effects of varying parameters on moving spins. The tubing was placed parallel to the magnetic field and perpendicular to the axial plane. Two portions of tubing were used, both with flow (sagittal sequences) or one with flow and one with air (axial sequences). A transmit/receive 17-cm linear extremity coil was used. Based on previous examinations of CSF pulsation in the cervical spine, the rates of flow were chosen to be 2 and 4 cm/sec (15, 16). The phantom was also run without flow for a control. The TR was 2000. The phase-encoding gradient was in the y-axis in the sagittal sequences, parallel to the flow, and in the y and z planes in the axial sequences, as in the clinical series.

Several experiments were conducted and are described in Table 3. The first experiment in either the sagittal or axial plane was chosen primarily to study the effect of echo spacing, and the second to examine the impact of echo train length, although experiments were repeated with different values of other parameters as well to cover different combinations of echo spacing and echo train length.

The images from all of the experiments were compared quantitatively and qualitatively. Quantitatively, region-of-interest measurements of the flow in the phantom, of the control, and of background were obtained with the same methodology as in the clinical analysis. Increasing phantom-to-background and phantom-to-control contrast indicated a relative increase in signal intensity of the phantom. Qualitatively, the images were examined for signal intensity and homogeneity of the flowing solution.

## Results

The results are shown in tabular form in Tables 4 and 5.

### Analysis—Sagittal Plane

Of the 23 patients studied, 5 were healthy; the other 18 had extradural disease at one or more

**TABLE 3: Phantom FSE pulse-sequence parameters**

| TR (msec) | TE (msec) | Echo Train Length | Echo Spacing (msec) |
|---|---|---|---|
| Sagittal | | | |
| 2000 | 14 or 56 | 4, 8, 12, 16 | 14 |
| 2000 | 14–28 or 120–130 | 16 | 14, 16, 18, 20, 22, 24, 26, 28[a] |
| Axial | | | |
| 2000 | 14–28 or 120–130 | 12 or 16 | 14, 16, 18, 20, 22, 24, 26, 28[a] |
| 2000 | 14 or 126 | 8, 12, 16 | 14 or 18 or 20 or 26 |

[a] 28 msec was not compatible with the long TE range.

**TABLE 4: Interaction of parameters and effects on imaging quality—sagittal plans**

| Parameters | Advantages | Disadvantages |
|---|---|---|
| ↑Echo train length | ↑Contrast | ↓SNR |
| | ↓Acquisition time | ↑Blurring |
| | ↓Motion artifact | ↓Number of sections for a given TR |
| | ↑Range of TE for a given echo spacing | ↑Truncation-type artifact[a] |
| | ↓Acquisition time per section | ↑Edge-enhancement artifact[a] |
| ↑Echo spacing | ↑Range of TE for a given echo train length | ↓Contrast |
| | | ↓SNR |
| | | ↑Blurring |
| | | ↑Magnetic susceptibility |
| | | ↑Motion artifact |
| | | ↑Acquisition time per section |
| | | ↓Number of sections for a given TR |
| | | ↑Truncation-type artiface |
| | | ↑Edge-enhancement artifact |

Note.—Tissues compared consisted of CSF, cord, disk, and spinal column.

[a] In this study not prominent because of phase-encoding gradient placed in y-axis.

**TABLE 5: Interaction of parameters and effects on imaging quality—axial plane**

| Parameter | Advantages | Disadvantages |
|---|---|---|
| ↑Echo train length | ↑Contrast | ↓SNR |
| | ↑Range of TE for a given echo spacing | ↑Blurring |
| | | ↑Truncation-type artifact |
| | | ↑Edge-enhancement artifact |
| | ↓Acquisition time | |
| ↑Echo spacing | ↑Range of TE for a given echo train length | ↓Contrast |
| | | ↓SNR |
| | | ↑Motion artifact |
| | | ↑Blurring |
| | | ↑Magnetic susceptibility |
| | | ↑Truncation-type artifact |
| | | ↑Edge-enhancement artifact |

Note.—Tissues compared consisted of CSF, cord, disk, and spinal column.

levels. Of these 18, 8 patients had disk protrusions, 6 had osteophyte formation, and 4 had combinations of these lesions. The influences of echo train length and echo spacing are discussed individually.

## Echo Train Length

CSF-to-cord contrast (Fig. 1) and CSF-to-disk contrast were mildly increased at long echo trains because of greater intensity of CSF. The SNR of cord decreased moderately with increasing echo train length, whereas the SNR of CSF decreased mildly (Fig. 2); therefore, the increase in contrast was due to a relative increase in signal of CSF rather than an absolute increase. Qualitatively, of the 12 patients studied with varying echo train lengths, pathology was seen in 8. These abnormalities were detectable regardless of the echo train length. Increasing homogeneity and signal intensity of CSF were seen with longer echo trains (Fig. 3). At a TE of 20, heterogeneity of CSF signal was seen with an echo train of 4 in 10



Fig. 3. A series of sagittal FSE images (2000/80) obtained with echo spacing of 20 while length of the echo train was varied from 4 (a) to 8 (b), 12 (c), and 16 (d). Note the increasing signal intensity of the CSF but a slight increase in blurring of lipid-containing tissues. Artifacts superimposed on the cord itself are due to aliasing in this case.
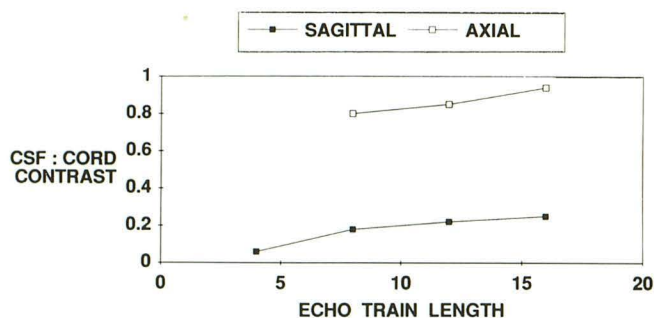


Fig. 1. Graph of CSF-to-cord contrast with increasing echo train length for both sagittal (2000/80) (TR/TE, echo spacing = 20) and axial (2000/126, echo spacing = 18) planes.
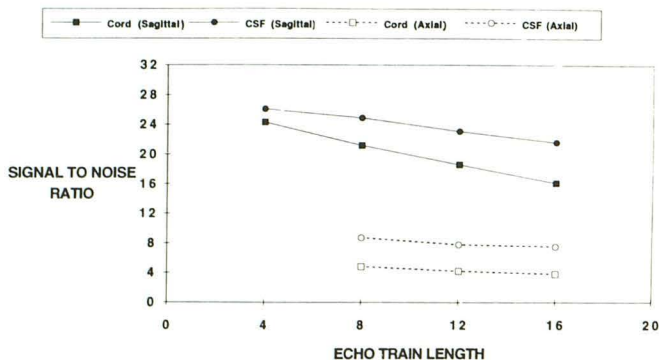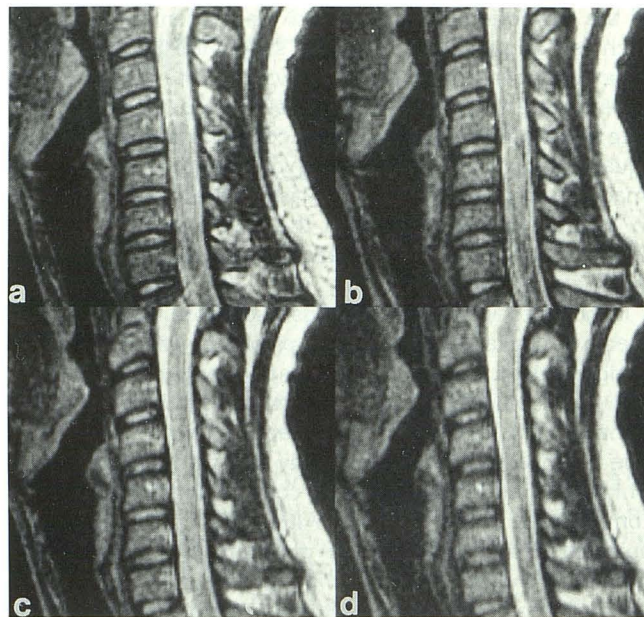


Fig. 2. Graph of SNR of CSF and cord with increasing echo train length for both sagittal and axial planes, using the same parameters as in Fig. 1.

patients. In 8 patients, significant heterogeneity was seen with an echo train of 8. In 7, heterogeneity was noted with an echo train of 12 and in 5 with an echo train of 16. At a TE of 80, heterogeneity of CSF signal was seen in 6 patients with an echo train of 4, in 5 patients with an echo train of 8, and in 4 patients with an echo train of either 12 or 16. A long echo train also decreased the time of each acquisition.

The use of longer echo trains, however, also had several disadvantages. Most importantly, increasing the length of the echo train increased the amount of blurring, especially on short TE images (Fig. 3). Structures with short T2 relaxation times, such as marrow lipid, were most susceptible to blurring. All images obtained with echo train lengths of 12 or 16 were found to suffer from significant blurring artifact on early echoes. Studies performed with an echo train length of 8 were found to suffer from minimal blurring artifact on early echoes; none had blurring on late echoes. Significant blurring artifact was not detected in any studies using an echo train of 4, regardless of TE. Of less importance for spinal imaging, increasing the length of the echo train also decreased the number of sections obtained for a given TR and decreased the time

of data acquisition for each section. Because it was difficult to avoid the blurring artifact and obtain homogeneous high-signal CSF in a single dual-echo acquisition, two separate single-echo sequences were chosen. An echo train of 8 was selected for the short TE sequence and an echo train of 16 for the long TE sequence. Because of increased blurring artifact with shorter TEs even with an echo train of 8, the optimal short TE was adjusted to the maximum in its range, approximately 40 in this study, which also increased CSF signal and permitted differentiation between CSF and cord.

### Echo Spacing

CSF-to-cord contrast (Fig. 4) and CSF-to-disk contrast decreased slightly with increased echo spacing. Minimal decreases in SNR of CSF or cord were detected (Fig. 5). Qualitatively, of the 11 patients studied using varying echo spacing, pathology was identified in 8 and was visualized with all echo spaces employed when long TEs were used. Myelographic effect, however, was decreased with longer echo spacing, especially at sites of epidural lesions (Fig. 6). In addition, lengthening the echo spacing was associated with increased blurring, motion, edge enhancement, and magnetic susceptibility artifacts and with a decreased number of sections for a given TR and increased acquisition time per section (Fig. 7). In the long TR/short TE sequence, using the values in the clinical trials, blurring was considered mild in studies performed with an echo spacing of 14. It was moderate in studies performed with an echo spacing of 16 or 18 and was severe in 8 of the 11 patients studied with an echo spacing of 20 and 22. In the long TR/long TE sequence, blurring was not significant in any studies per-



Fig. 5. Graph of SNR of CSF and cord with increasing echo spacing for both sagittal and axial planes, using the same parameters as in Fig. 4.



Fig. 6. A series of sagittal FSE images (2000/120–132) obtained with echo train length of 16. Echo spacings were varied from 14 (a) to 16 (b), 18 (c), 20 (d), and 22 (e). Note decreasing homogeneity and signal of CSF, especially where movement of CSF is increased at areas of disks.
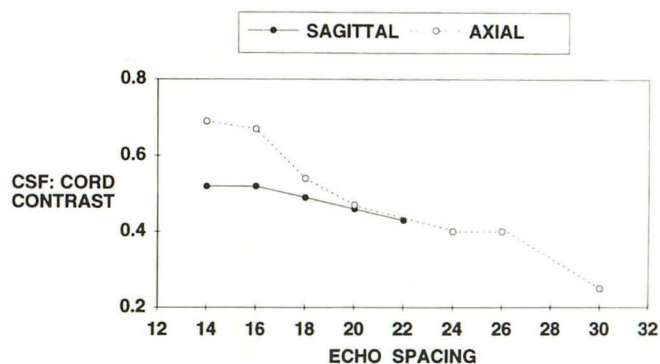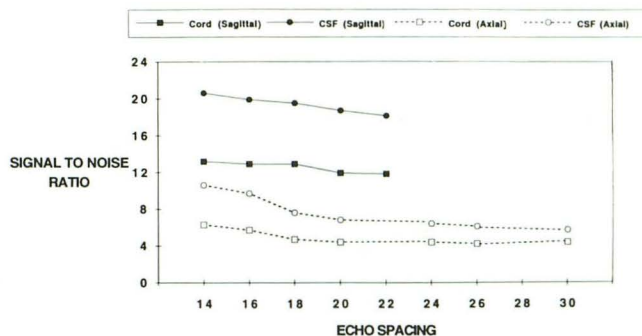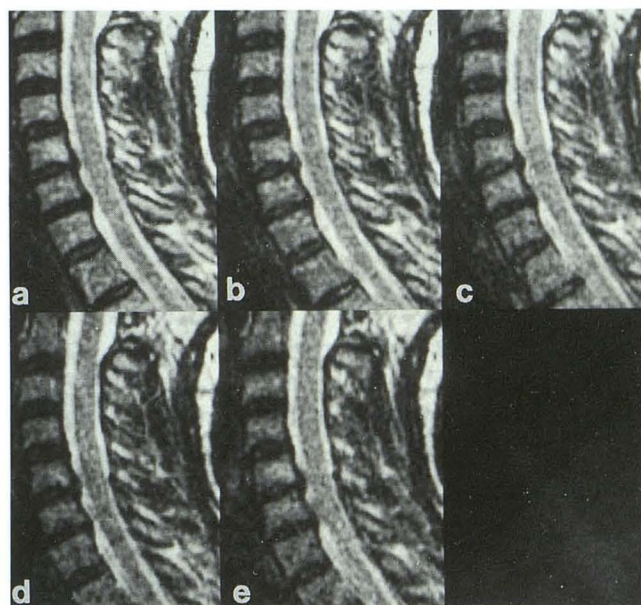


Fig. 4. Graph of CSF-to-cord contrast with increasing echo spacing for both sagittal (2000/120–132, echo train length = 16) and axial (2000/120–130, echo train length = 16) planes.

formed with an echo spacing of 14, 16, or 18. It was considered significant in 2 of the 11 patients studied with an echo spacing of 20 and 22. In addition, increasing echo spacing produced greater motion artifact and greater edge enhancement artifact, detected as a low intensity outlining the cord and other structures (Fig. 7). Of less importance for spinal imaging, increasing the echo spacing also decreased the number of sections obtained for a given TR and increased the time of acquisition for each section.

Increasing the echo spacing appeared to have only one single benefit: it increased the range of
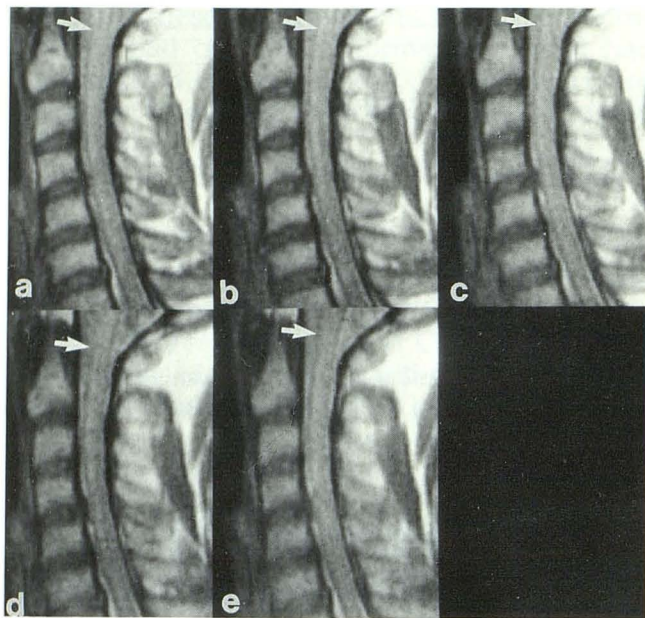
Fig. 7. A series of sagittal FSE images obtained with a TR of 2000, echo train length of 16, and TE from 14 to 22. Echo spacings were varied from 14 (*a*) to 16 (*b*), 18 (*c*), 20 (*d*), and 22 (*e*). Note increasing blurring and edge enhancement artifact (*arrows*).

the TE if a short echo train was used, because the maximum TE permissible was AB, where A is the number of echoes in the echo train, and B is the interecho spacing. For the maximum TE, the lowest order phase encodes were placed on the final echo of the echo train.

For spin-density images, a relatively short TE eliminated the necessity for a longer echo spacing. The optimal echo spacing was selected to be short, 14 msec in this study, to decrease artifacts. In heavily T2-weighted images, with long TEs, the optimal echo spacing was also short (14 msec) because of the benefits of the decreased echo spacing and because the long echo train (16) in this acquisition allowed long TEs (up to 224).

## Analysis—Axial Plane

Of the 18 patients studied, 4 were healthy; fourteen had extradural disease at one or more levels. Seven had osteophyte formation resulting in impingement on either the spinal canal centrally or on the neural foramina, 4 had disk protrusion, and 3 had a combination of these lesions. The influences of echo train length and echo spacing are discussed individually.

## Echo Train Length

Increases in CSF-to-cord contrast (Fig. 1) or CSF-to-disk contrast were seen with increasing echo train length. The SNRs of cord and CSF were slightly better at lower echo trains (Fig. 2). Of the 10 patients examined with varying lengths of the echo train, pathology was seen in 7 and was visible with all the echo train lengths varied here at the long TEs. Homogeneity and intensity of the CSF signal was slightly improved with longer echo trains (Fig. 8). Longer echo trains also were associated with a minimal increase in truncation-type and edge-enhancement artifacts surrounding the cord, described more fully in the next section. As in the sagittal plane, however, the shorter echo trains limited the use of longer TEs and increased acquisition time. Therefore, the optimal echo train length was selected to be moderately long (12) in this study.

As in the sagittal plane, the use of longer echo trains increased the amount of blurring. Again, short TE sequences and structures with short T2 relaxation times were most affected. On the long TE sequences which produced the high-intensity CSF, however, blurring artifact was not significant. None of the 10 patients examined with a TE of 126 with the brief echo spacing of 14 or 18 msec and with varying echo trains was found to show significant blurring artifact.

## Echo Spacing

Decrease in CSF-to-cord contrast (Fig. 4) and CSF-to-disk contrast were seen with increased echo spacing. The SNR of CSF and cord also decreased slightly (Fig. 5). Of the eight patients examined with varying echo spacing, pathology was seen in three at the long TEs. Lesions were visible in all patients with an echo spacing of 14, 16, or 18 msec, in six of eight with an echo spacing of 20, 22, or 24 msec, and in five of eight with an echo spacing of 26 or 30 msec.

An increase in motion artifact was seen with increased echo spacing (Fig. 9). This effect was most prominent as a result of vascular flow, with ghost images propagating in the in-plane phase-encoding direction. Additional motion artifact was also created, though to a lesser extent, by CSF pulsation. As a result, increasing echo spacing led to image degradation from motion artifact and to decreased signal intensity of the CSF. These effects were prominent in all patients in group 4.
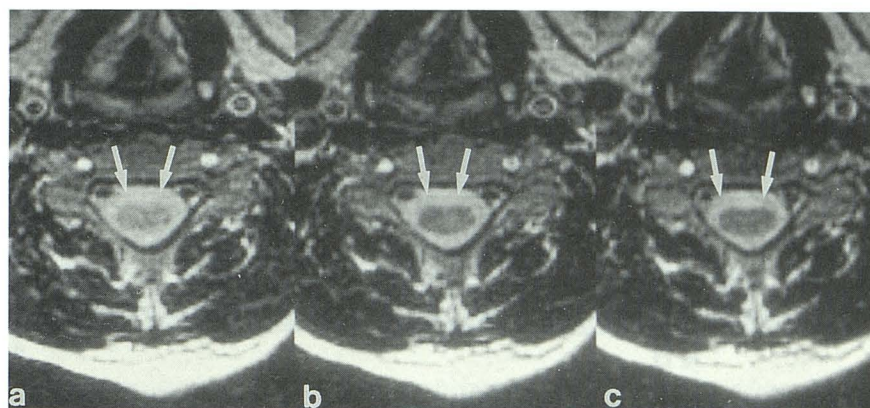
Fig. 8. A series of axial images (2000/126) obtained with echo spacing of 14 and echo train of 8 (a), 12 (b), or 16 (c). Note increasing CSF-to-cord contrast and a slight increase in truncation-type artifact (arrow).
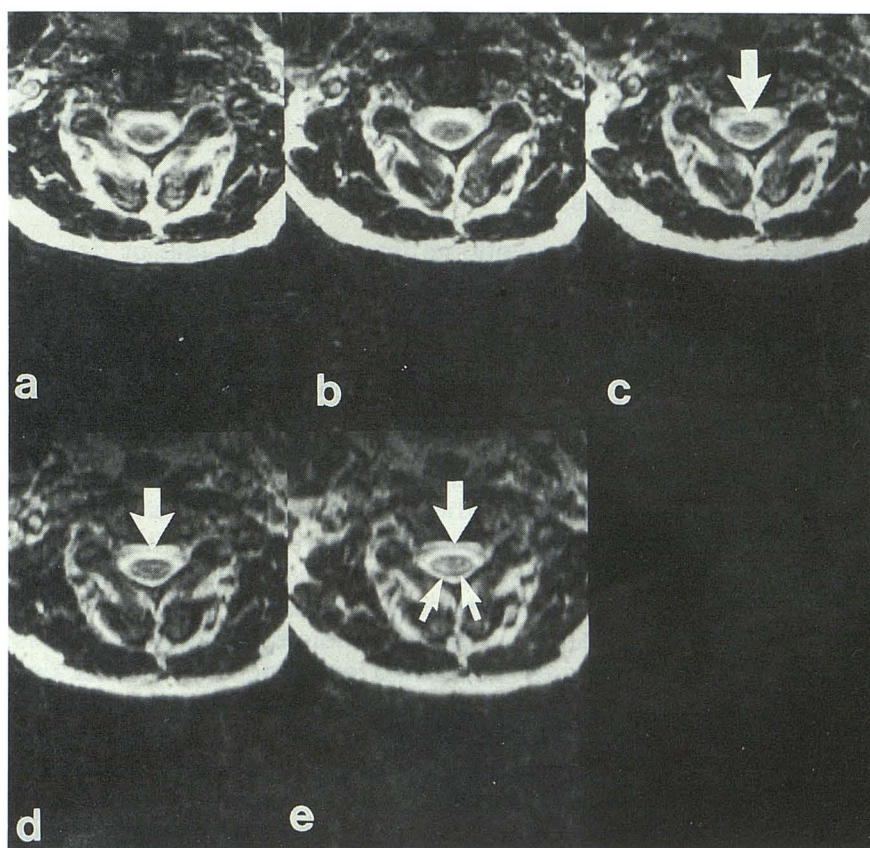


Fig. 9. A series of axial images (2000/120–130) obtained with echo train length of 16. The echo spacing varied from 14 (a) to 16 (b), 20 (c), 24 (d), and 26 (e). Note decreased signal intensity and homogeneity of CSF signal with increasing echo spacing. Note increasing edge enhancement (arrows) and truncation-type artifact (arrowheads). Both occur perpendicular to the phase-encoding direction and were switched to left-right when phase encoding was also switched. Also note increasing motion artifact propagating along the phase-encoding direction from the vessels.

An increase in edge-enhancement and truncation-type artifacts was also seen with increased echo spacing (Fig. 9). Edge enhancement occurred because of a dark border surrounding the cord. Truncation-type artifact was manifested by lines of low signal intensity in the CSF, parallel to the CSF-to-vertebra interface, perpendicular to the phase-encoding direction. A slight increase in blurring artifact and in magnetic-susceptibility artifact were seen with increased echo spacing. Again, blurring artifact was not significant regardless of echo spacing when long TEs were used.

The increased magnetic-susceptibility artifact led to a mild increase in the apparent size of degenerative changes, especially of the neural foramina, in two of the eight patients. Because of the problem with artifacts, the optimal echo spacing was felt to be short, 14 msec in this study.

Flow Phantom

The relationship between image contrast and echo train length or echo spacing was confirmed in the flow phantom (Figs. 10 and 11). In the
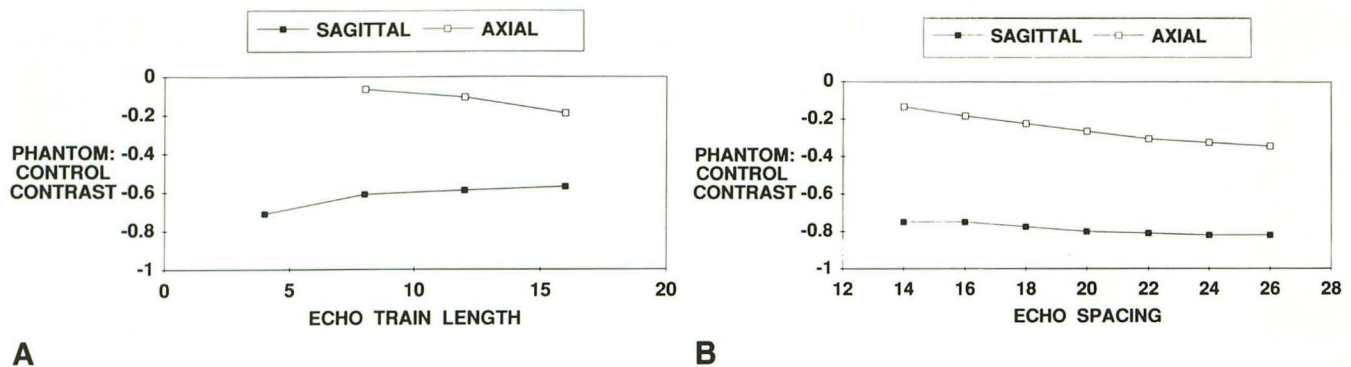
Fig. 10. *a*, Graph of phantom-to-control contrast with increasing echo train for both sagittal and axial planes.
*b*, Graph of phantom-to-control contrast with increasing echo spacing for both sagittal and axial planes.

sagittal plane, when echo train was increased (from 4, 8, 12 to 16), phantom-to-background and phantom-to-control contrast increased. Qualitatively, these findings were reflected in the increased signal intensity and homogeneity in the phantom. When echo spacing was increased (from 14, 16, 18, 20, 22, or 24 to 26), phantom-to-background and phantom-to-control contrast decreased, consistent with decreasing signal intensity and homogeneity in the phantom. These findings were similar to those seen in the clinical series. With both echo train length and echo spacing, the effects were more pronounced at higher flow rates. The control bath SNR decreased slightly with increases in echo train and echo spacing.

In the axial plane, when echo train length was increased (from 8 or 12 to 16), phantom-to-background and phantom-to-control contrast decreased. Qualitatively, signal intensity and homogeneity in the phantom decreased slightly. These findings were the reverse of those seen in the sagittal plane or in the clinical series. When the echo spacing was increased (from 14, 18, 20, 22, or 26 to 28), phantom-to-background and phantom-to-control contrast decreased. Qualitatively, signal intensity and homogeneity in the phantom decreased. In addition, increased motion, edge enhancement, and truncation-type artifacts in the in-plane phase-encoding direction were seen. These findings were similar to those seen in the clinical series.

In all cases in the axial plane, increased signal was noted in the sections from the outer peripheral slabs and in the outer peripheral sections within each slab, because of inflow phenomena. Finally, signal was also increased in inflow arms

of the phantom in which previously unsaturated spins entered.

## Discussion

In conventional imaging, each line of data in the $k_y$ direction is acquired at the same TE; k-space ordering does not impact on image quality, excluding the effects of motion artifacts. In routine SE imaging, contrast is primarily controlled by TR and TE. In gradient-echo imaging, contrast is governed primarily by flip angle, with TR and TE contributing to a lesser extent. In FSE imaging, however, the order in which k-space is sampled becomes critical in imaging contrast and is reflected in the new FSE parameters, echo train length, echo spacing, and the TE.

The range of parameters examined in this study was chosen to examine all practical options. Echo trains shorter than those used here were not attempted, because they would prolong imaging time over the time required for routine gradient-echo images and thus were considered unsatisfactory. As in SE imaging, the time of each acquisition was directly proportional to the TR, the number of excitations, and the number of phase-encoding steps, and was inversely proportional to the number of phase-encoding steps per TR. In FSE imaging, the number of phase-encoding steps per TR was equal to the number of echoes in the echo train. In other groups, ranges of TE, rather than a single value, were used when the echo spacing was varied; identical TEs could not be used with different echo spacing, because the precise value of TE must be a multiple of the value of the echo spacing. Longer echo spacing up to 40 msec was employed in three patients but discontinued, because it was
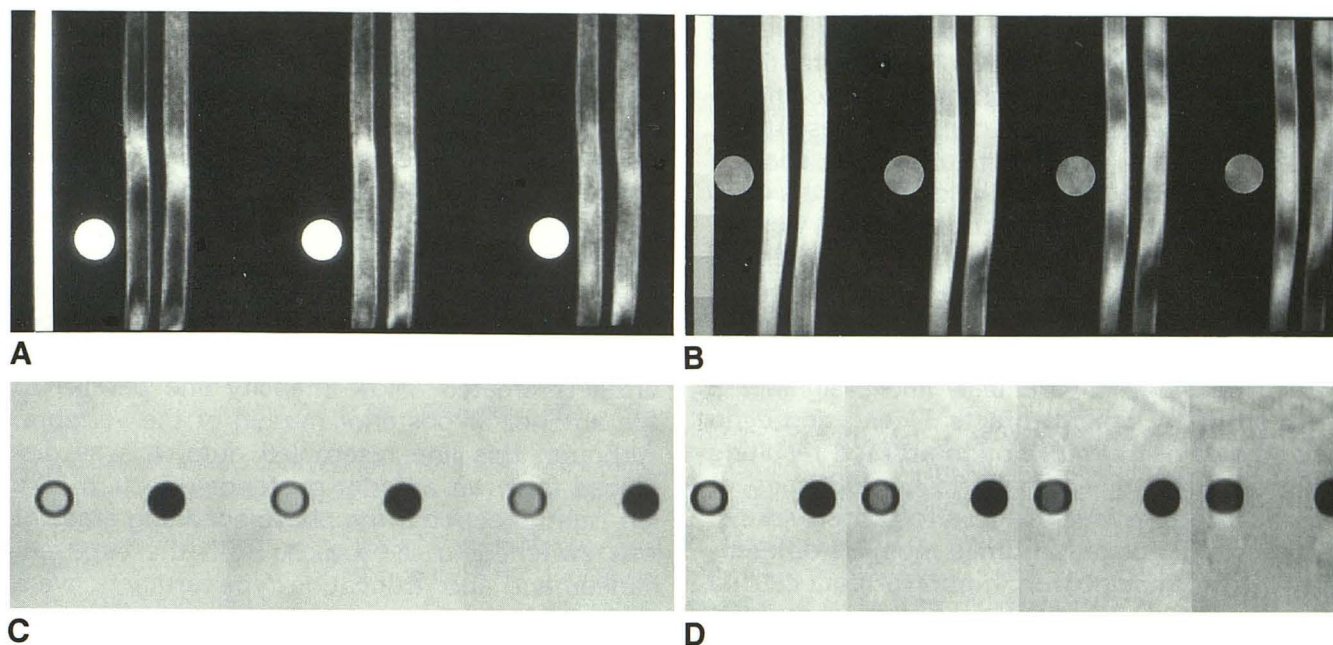
Fig. 11. Flow phantom. In the sagittal plane (*a*), increasing echo train lengths of 4, 8, and 16 are associated with increasing signal intensity and homogeneity of both tubes, whereas (*b*) increasing echo spacing of 14, 18, 22, and 26 produces decreasing signal. Circular container of control solution is seen on each section. In the axial plane (*c*), increasing echo train lengths of 8, 12, and 16 show decreasing signal of flow tube on left, whereas (*d*) increasing echo spacing of 14, 18, 22, and 26 discloses decreasing signal and increasing motion, edge enhancement, and truncation-type artifacts in the phase-encoding direction. Control solution surrounds the flow tube (*left*) and air-filled tube (*right*).

noted immediately to decrease the number of sections for a given TR, increase blurring artifact, and decrease contrast.

2DFT FSE sequences were not extensively tested in the axial plane in this study, because they sometimes failed to produce significant CSF signal in pilot studies despite extensive manipulation of parameters. This observation followed closely from the experience with routine SE imaging. Although flow-related enhancement can contribute to signal in the axial plane, the marked pulsatility of CSF can also produce wash-out of spins and phase shift effects that disrupt the homogeneity of the CSF signal (9–12). The 3DFT FSE sequences were able both to achieve high-intensity CSF signal and to allow acquisition of sections as thin as 1 mm, a capability of significant potential in imaging cervical spine disk disease.

Although the contributions of TR and TE to contrast resembled those of SE, the impact of the new FSE parameters, echo train length, and echo spacing on image contrast and SNR were more difficult to predict intuitively. However, the new parameters were significant, because typical parameters of SE imaging often failed to produce satisfactory images when the FSE sequences were employed. Longer echo trains and shorter echo spacing were associated with an increase in CSF-to-disk and CSF-to-cord contrast in both the 2DFT and 3DFT sequences. These effects may have been partially caused by the rephasing effect of rapid repeated 180° pulses on the moving protons in the CSF. The difference in clinical findings from those of the phantom in the axial 3DFT sequence with regard to echo train length could only have been caused by the to-and-fro motion of CSF pulsation, as opposed to the unidirectional movement of the flow phantom, because it would permit protons to reenter the imaging plane. This contribution would be accentuated with longer echo trains. Further studies regarding the interaction of these parameters with the effects of flow are underway.

Although the echo train length and echo spacing were found to contribute to contrast, use of these parameters to maximize contrast was limited, to some extent, by the appearance of certain artifacts, blurring in particular. Decreases in echo train length and echo spacing minimized T2 at-

tenuation differences throughout the echo train and thus decreased blurring artifact substantially. The echoes to which the high-order phase-encoding gradients were applied controlled resolution. Hence, a shorter echo train and echo spacing reduced the T2 decay over the course of the echo train and reduced T2 blurring. Blurring was increased with short TEs because of placement of the high-order spatial frequencies that control resolution further from the 90° pulse, resulting in greater $T_2$ decay (17, 18).

Echo spacing, in particular, had a significant effect on many other artifacts. Decreasing echo spacing also decreased motion artifact, resulting in increased relative signal and homogeneity of CSF. Blurring artifact which affected structures with short T2 relaxation times must be differentiated in FSE imaging from motion artifact caused by moving spins. Magnetic-susceptibility artifact, due to diffusion-related dephasing phenomena, as in SE imaging, was noted to decrease with shorter echo spacing. The effect has been related to lengthening of T2 with decreasing echo spacing. For the evaluation of suspected degenerative change, this reduction of artifact was felt to be beneficial for the assessment of patients with prominent hypertrophic osteophytes and of patients in the postoperative, because prominent susceptibility-induced effects may lead to overestimation of degenerative changes. Whether the decreased artifact will compromise the detection of hemorrhagic cord lesions lies outside of the scope of this study. Finally, a short echo spacing diminished the edge-enhancement artifact, noted as decreased signal intensity outlining the cord periphery, and the truncation-type artifact, seen as banding parallel to interfaces of two tissues with different T2 values. Edge-enhancement artifact has been attributed to T2 decay during data collection and can be manifested as increased or decreased signal. Artifacts resembling conventional truncation artifacts are seen with FSE imaging and were termed truncation-type artifacts in this study. Although the standard truncation artifact results from sine-function–type oscillations due to the Fourier transformation (19–21), the truncation-type artifacts of FSE imaging were caused by the combination of T2 relaxation processes and discontinuities of the k-space trajectory (17, 22). Different echo numbers have discrete T2 decay values, leading to discontinuities in the T2 decay function from echo to echo. (If the echo spacing were 0, then there would be no discontinuities in the T2 decay-weighting function.) Like standard truncation artifacts, they were most prominent perpendicular to the phase-encoding direction. In this study, the phase-encoding axis was parallel to the spine in the sagittal plane, minimizing the effects of these artifacts. In the axial plane, however, the truncation-type artifacts were visible as low-intensity bands in the CSF and were minimally increased with increasing echo-train length and markedly increased with increasing echo spacing. With the phase-encoding gradients in the y-axis, the truncation-type artifacts created a low-intensity line parallel to the anterior or posterior margin of the vertebra. Although this line resembled dura, it was displaced from an anterior-posterior direction to a left-right direction if the phase-encoding gradient was switched to the x-axis. Both the edge enhancement and truncation-type artifacts were also visible in the phantom when no flow was used, confirming that they were not due to CSF pulsation.

Attainment of reliably high-intensity CSF signal was difficult, possibly due to the absence of cardiac gating. Although cardiac gating could be implemented with FSE sequences, the acquisition time greatly lengthened, eliminating much of the advantage of this sequence. In addition, gradient moment nulling was not used in the optimization of parameters in order not to limit the range of variables, because the brief time period between 180° pulses compromised the addition of extra gradient pulses, and implementation of gradient moment nulling techniques sometimes required minimal prolongation of the interecho spacing.

In conclusion, the effects of echo train length and echo spacing and the interaction of these parameters with image contrast, CSF flow, artifact production, and acquisition speed are complex. Optimal production of high-intensity CSF requires maximization of echo train length within allowable limits of artifact production and minimization of echo spacing within technical capabilities.

## References

1. Hennig J, Naureth A, Friedburg H. RARE imaging: a fast imaging method for clinical MR. *Magn Reson Med* 1986;3:823–833
2. Hennig J, Friedburg H, Strobel B. Rapid nontomographic approach for MR myelography without contrast agents. *J Comput Assist Tomogr* 1986;10:375–378
3. Hennig J, Friedburg H, Ott D. Fast three-dimensional imaging of cerebrospinal fluid. *Magn Reson Med* 1987;5:380–383

4. Hennig J, Friedburg H. Clinical applications and methological developments of the RARE technique. *Magn Reson Imaging* 1988;6:391–395

5. Mulkern RV, Wong STS, Winalski C, Jolesz FA. Contrast manipulation and artifact assessment of 2D and 3D RARE sequences. *Magn Reson Imaging* 1990;8:557–566

6. Melki PS, Mulkern RV, Panych LP, Jolesz FA. Comparing the FAISE method with conventional dual-echo sequences. *J Magn Reson Imaging* 1991;1:319–326

7. Oshio K, Jolesz FA, Melki PS, Mulkern RV. T2-weighted thin-section imaging with the multislab three-dimensional RARE technique. *J Magnetic Reson Imaging* 1991;1:695–700

8. Tsuruda JS, Remley K. Effects of magnetic susceptibility artifacts and motion in evaluating the cervical neural foramina in 3DFT gradient-echo MR imaging. *AJNR: Am J Neuroradiol* 1991;12:237–241

9. Enzmann DR, Rubin JB. Cervical spine: MR imaging with a partial flip angle, gradient-refocused pulse sequence. Part I. General considerations and disk disease. *Radiology* 1988;166:467–472

10. Hedberg MC, Drayer BP, Flom RA, Hodak JA, Bird CR. Gradient echo (GRASS) MR imaging in cervical radiculopathy. *AJNR: Am J Neuroradiol* 1988;9:145–151

11. Van Dyke C, Ross JS, Tkach J, Masaryk TJ, Modic MT. Gradient-echo MR imaging of the cervical spine: evaluation of extradural disease. *AJNR: Am J Neuroradiol* 1989;10:627–632

12. Tsuruda JS, Norman D, Dillon W, Newton T, Mills D. Three-dimensional gradient-recalled MR imaging as a screening tool for the diagnosis of cervical radiculopathy. *AJNR: Am J Neuroradiol* 1989;10:1263–1271

13. Enzmann DR, O'Donohue J. Optimizing MRI for detection of small tumors in the CPA and IAC. *AJNR: Am J Neuroradiol* 1987;8:99–106

14. Jones KM, Mulkern RV, Mantello MT, et al. Brain hemorrhage: evaluation with fast spin-echo and conventional dual spin-echo images. *Radiology* 1992;182:53–58

15. Quencer RM, Donovan Post MJ, Hinks RS. Cine MR in the evaluation of normal and abnormal CSF flow: intracranial and intraspinal studies. *Neuroradiology* 1990;32:371–391

16. Enzmann DR, Pelc NJ. Normal flow patterns of intracranial and spinal CSF defined with phase-contrast cine MR imaging. *Radiology* 1991;178:467–474

17. Constable RT, Gore JC. The loss of small objects in variable TE imaging: Implications for FSE, RARE, and EPI. *Magn Reson Med* (in press)

18. Constable RT, Anderson AW, Zhong J, Gore JC. Factors influencing contrast in FSE MR imaging. *Magn Reson Imaging* 1992;10:497–511

19. Czervionke L, Czervionke J, Daniels D, Haughton V. Characteristic features of MR truncation artifacts. *AJNR: Am J Neuroradiol* 1988;9:824–824

20. Breger R, Czervionke L, Kass E, et al. Truncation artifact in MR images of the intervertebral disk. *AJNR: Am J Neuroradiol* 1988;9:825–828

21. Yousem D, Janik P, Atlas S, et al. Pseudoatrophy of the cervical portion of the spinal cord on MR images: a manifestation of the truncation artifact? *AJNR: Am J Neuroradiol* 1990;11:373–377

22. Mulkern RV, Melki PS, Jakab P, Higuchi N, Jolesz FA. Phase-encode order and its effect on contrast and artifact in single-shot RARE sequences. *Med Phys* 1991;18:1032–1037